Optics & Laser Technology 72 (2015) 65–69

Contents lists available at ScienceDirect

Optics & Laser Technology

journal homepage: www.elsevier.com/locate/optlastec

An in-line quasi-Sagnac interferometer based comb filter used for tunable multi-wavelength fiber laser

Hao Sun [a], Jing Zhang [a,b], Zaihang Yang [a], Libin Zhou [a], Xueguang Qiao [a], Manli Hu [a,*]

[a] School of Physics, Northwest University, No. 229, Taibai Road, Beilin District, Xi'an, Shaanxi 710069, China
[b] Photonics Research Group, Center for Nano and Biophotonics, Ghent University-imec, Ghent 9000, Belgium

ARTICLE INFO

Article history:
Received 16 December 2014
Received in revised form
11 March 2015
Accepted 31 March 2015
Available online 16 April 2015

Keywords:
Fiber laser
Comb filter
Sagnac interferometer

ABSTRACT

An in-line quasi-Sagnac interferometer comb filter based on high birefringence (Hi-Bi) fiber is proposed and experimentally demonstrated. This quasi-Sagnac interferometer is constructed by integrating a high-birefringence (Hi-Bi) fiber in between two fiber-coupled polarization controllers (PCs) followed by a fiber mirror. The filtering function is theoretically analyzed and simulated by the Jones matrix method. The extinction ratio and wavelength interval of the output spectrum can be flexibly adjusted by rotating the PCs. By only using a pump light source and gain medium, stable multi-wavelength lasing operation can be realized at room temperature. These advantages of tunable ability, switchable ability and good stability make the proposed filter to have broad application prospects in the field of tunable multi-wavelength fiber laser.

1. Introduction

Multi-wavelength fiber lasers have attracted continuous attention due to their potential applications in wavelength division multiplexing (WDM) system, optical sensing, instrument testing, optical communications and spectroscopy [1–4]. For realizing multi-wavelength oscillation, a comb filter is indispensable in laser cavities. Initially, fiber Bragg grating (FGB), long period fiber grating (LPG), arrayed waveguide grating (AWG) or cascaded FBGs were employed to select lasing wavelength [5–6]. Generally, in order to achieve multiple lasing lines simultaneously, a certain number of FBGs is required and this will result in a complex configuration. Thus some interferometer filters used as wavelength selection components in the design of multi-wavelength fiber lasers have been developed and reported *e.g.* Fabry–Perot interferometer (FPI), Mach–Zehnder interferometer (MZI) and fiber loop mirror (FLM) based Sagnac interferometer [7–9]. The fiber lasers based on an FP tunable cavity formed by incorporating with piezoelectric stack actuators or an MZI incorporating optical variable delay line can achieve multi-wavelength tunable operation effectively. The FLM with multi-section Hi-Bi fibers and corresponding PCs have also been reported to realize multi-wavelength lasing operation with more flexible tunable and switchable ability [10], but the multiple Hi-Bi fibers and PCs incorporated in the FLM make the layout rather complex.

In recent years, researchers proposed some new technology and new components to choose wavelength and construct fiber lasers. Bergeron et al. demonstrated that the silica micro-disk resonator filters could be used to control the spectral emission of an erbium doped fiber (EDF) laser [11]. By modifying the number and sizes of the micro-disks, both single and multiple wavelength lasing output were realized. Mamdoohi et al. demonstrated a single-spacing, multi-wavelength Brillouin–Raman fiber laser using an enhanced nonlinear amplifying loop mirror cavity [12]. In this structure, up to 28 channels with an average 17 dB signal-to-noise ratio (SNR) were achieved. Jhang et al. reported a switchable multi-wavelength fiber ring laser based on a weak resonant cavity Fabry–Perot laser diode [13]. The lasing wavelength of this multi-wavelength laser can be flexibly switched in the C-band and L-band.

In this paper, an in-line quasi-Sagnac interferometer based comb filter is proposed and demonstrated. The filtering function is theoretically analyzed and simulated by the Jones matrix method, which is also confirmed by the experimental results. The interferometer is then inserted into an EDF laser ring cavity containing a semiconductor optical amplifier (SOA). The EDF can provide high gain and the SOA can improve the mode suppression ratio. Up to 14 lasing lines operation with an average 40 dB SNR has been realized by exploiting this inline Sagnac interferometer as the comb filter.

2. Experiment setup and principle

As shown in Fig. 1, the in-line quasi-Sagnac interferometer consists of polarizer, PCs, Hi-Bi fiber and mirror. The extinction ratio of

* Corresponding author.
E-mail address: huml@nwu.edu.cn (M. Hu).

http://dx.doi.org/10.1016/j.optlastec.2015.03.017
0030-3992/

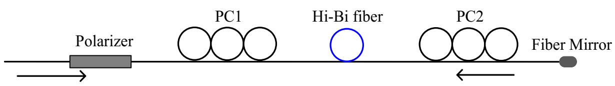

Fig. 1. The schematic setup of the in-line quasi-Sagnac interferometer.

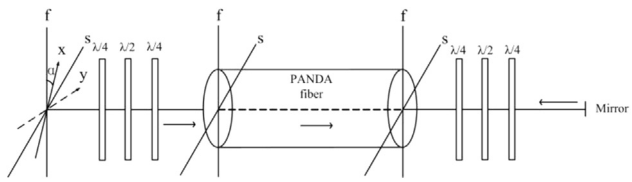

Fig. 2. Illustration of the polarization state of the propagation light in the quasi-Sagnac interferometer.

the used normal SMF polarizer is about 30 dB. Two commercial polarization controllers are formed by sandwiching a half wave plate fiber coil between two quarter plates fiber coils. The birefringence specified by manufacturer of the Hi-Bi fiber is 6.24×10^{-4} and the reflectivity of fiber mirror is about 98%.

The polarization state of the propagation light in the quasi-Sagnac interferometer is schematically illustrated in Fig. 2. Suppose that the polarizer at an angle of α with respect to the vertical birefringence axis f. The Jones Matrix of the linearly polarization light output from the polarizer can be represented as [14] follows:

$$J_P = \begin{pmatrix} \cos\alpha & \sin\alpha \\ -\sin\alpha & \cos\alpha \end{pmatrix} \begin{pmatrix} E_x \\ 0 \end{pmatrix}, \tag{1}$$

where E_x is the amplitude of the polarization light output from the polarizer. For simplifying the calculation, we assume $\alpha = 0$. With E'_x and E'_y denoting the amplitudes of the light objected on the two orthogonal axes x and y (see Fig. 2), the transmission characteristics of this filter can be analyzed by the following Jones Matrix representation:

$$\begin{pmatrix} E'_x \\ E'_y \end{pmatrix} = J'_{PC1} J_{Hi-Bi} J'_{PC2} J_M J_{PC2} J_{Hi-Bi} J_{PC1} \begin{pmatrix} E_x \\ 0 \end{pmatrix}, \tag{2}$$

where J_{Hi-Bi} and J_M represent the matrices of Hi-Bi fiber and fiber mirror, respectively. Then we can obtain the following:

$$J_{Hi-Bi} = \begin{pmatrix} 1 & 0 \\ 0 & e^{i\Delta\varphi} \end{pmatrix}, \tag{3}$$

$$J_M = \begin{pmatrix} 1 & 0 \\ 0 & 1 \end{pmatrix}. \tag{4}$$

where $\Delta\varphi = 2\pi\Delta nL/\lambda$ is the phase shift between two orthogonal modes. Δn, L and λ are the birefringence, the length of Hi-Bi fiber and the operation wavelength, respectively.

In Eq. (2), J_{PCn} (n=1, 2) represents the Jones matrix of the PCs. J'_{PCn} denotes the matrix of the PC as the light reverse in reverse order. For the used PCs with three plates, the transmission matrix can be written as $J_{PCn} = \sum T(\theta_j)$, and the transmission matrices of the three plates can be expressed as follows:

$$T_{(\theta_j)} = \begin{pmatrix} \cos\frac{\varphi_j}{2} + i\sin\frac{\varphi_j}{2}\cos 2\theta_j & i\sin\frac{\varphi_j}{2}\sin 2\theta_j \\ i\sin\frac{\varphi_j}{2}\sin 2\theta_j & \cos\frac{\varphi_j}{2} - i\sin\frac{\varphi_j}{2}\cos 2\theta_j \end{pmatrix}, \tag{5}$$

where θ_j ($j = 1, 2, 3$) represents the angles induced by rotating these three plates. $\varphi_1 = \pi/2$, $\varphi_2 = \pi$ and $\varphi_3 = \pi/2$ correspond to the three wave plates. With $T(\lambda)$ denoting the final transmission of the interferometer configuration, it can be obtained as the following:

$$T(\lambda) = \frac{|E'_x|^2}{|E_x|^2}. \tag{6}$$

For further investigation on the interference function and spectral characteristics, the wavelength interval between two adjacent interference peaks can be expressed as $\Delta\lambda = \lambda^2/(2L\cdot\Delta n)$ according to the phase matching condition of interference. As can be seen from this equation, the wavelength interval is proportional to operating wavelength, and inversely proportional to Hi-Bi fiber's length and birefringence. The longer Hi-Bi fiber can get narrower wavelength interval in interference spectrum. While for the proposed interferometer, the wavelength interval depends on both the Hi-Bi fiber and the PCs. The side frequencies can be restrained by choosing appropriate length of the Hi-Bi fiber [14]. Considering the two factors of wavelength interval and side frequency, a section of 50 cm Hi-Bi fiber was used in the filter configuration. The resonant wavelengths λ' *i.e.* interference peak wavelengths satisfy $(4\pi L\Delta n + \beta)/\lambda' = 2k\pi$, where k is any integer and β is a constant of phase difference induced by polarization angle. For simplifying the calculation, we suppose $\beta = 0$, thus the positions of the interference peaks are determined by $\lambda' = 2BL/k$. Thus it can be seen that the transmission characteristics of this quasi-Sagnac interferometer are similar to those Sagnac interferometers based on Hi-Bi FLM.

Based on above theoretical result, we simulated the interference characteristics of the proposed interferometer with different parameters. The states of the PCs play an important role in characteristics of the in-line quasi-Sagnac interferometer. We plot 3-D figures of the transmission spectra with θ_{ij} changing from $-\pi/2$ to $\pi/2$. The simulated spectra are shown in Figs. 3 and 4, of which the length of Hi-Bi fiber is 50 cm and the birefringence specified by manufacturer is 6.24×10^{-4}, where the PC1 states are set to be (a) $(\theta_{11},\pi/6,\pi/3)$, (b) $(\pi/8,\theta_{12},\pi/4)$, and (c) $(\pi/6,\pi/9,\theta_{13})$ in Fig. 3(a, b and c), respectively, while the PC2 state is $(\pi/8,\pi/4,\pi/8)$. In Fig. 4, PC1 is under the state of $(\pi/9,\pi/5,\pi/9)$ and PC2 states are set to be (a) $(\theta_{21},\pi/4,\pi/8)$, (b) $(\pi/3,\theta_{22},\pi/6)$, and (c) $(\pi/4,\pi/4,\theta_{23})$.

In the plate angle-axes direction, the spectrum has a wavelength interval of about 8.3 nm, the fringe phase varies with the rotation angle, and then the wavelength interval gradually changes between 8.3 nm and a half of that value. As depicted in Figs. 3(c) and 4(c), the wavelength interval also exhibits a variation with the rotation angle, but the invisible fringe shows a remarkable change during the course. As the half wave plates vary, the fringes exhibit blue-shift, but there is no impact on visibility and the wavelength spacing. It can be seen from the simulation that the spectral response of the proposed in-line quasi-Sagnac interferometer is rather variable, and the expected interference spectra can be obtained by adjusting the wave plates of the PCs.

3. Experimental results and discussion

The filtering characteristics of the in-line quasi-Sagnac interferometer were tested firstly. A section of 0.5 m Hi-Bi fiber with the birefringence of 6.24×10^{-4} was incorporated in this interferometer. For testing the spectra, a fiber circulator was used to guide an ASE source to the interferometer device, and the reflected light was guided out through the output port of the circulator to an optical spectrum analyzer (OSA) (YOKOGAWA AQ6370B) with the resolution of 0.02 nm. To our knowledge, Hi-Bi fiber has two axes (fast and slow channels) that support the propagation of two orthogonal polarization modes in the fiber with a high isolation. The phase delay between the two orthogonal modes in Hi-Bi fiber could cause an optical path difference and induce an interference fringe. For this reason, a unique interference pattern can be expected in the reflection spectrum of the proposed interferometer. Due to the reflection